

1 **Climate change drives uncertain global shifts in potential distribution and seasonal risk of**  
2 ***Aedes*-transmitted viruses**

3

4 Sadie J. Ryan<sup>1,2,3\*†</sup>, Colin J. Carlson<sup>4\*</sup>, Erin A. Mordecai<sup>5</sup>, Leah R. Johnson<sup>6</sup>

5

6 **Affiliations:**

7 <sup>1</sup>Department of Geography, University of Florida, Gainesville, Florida, United States of America

8 <sup>2</sup>Emerging Pathogens Institute, University of Florida, Gainesville, Florida, United States of  
9 America

10 <sup>3</sup>School of Life Sciences, University of KwaZulu-Natal, Durban, South Africa

11 <sup>4</sup>Department of Environmental Science, Policy, and Management, University of California,  
12 Berkeley, 130 Mulford Hall, Berkeley, California, United States of America

13 <sup>5</sup>Department of Biology, Stanford University, 371 Serra Mall, Stanford, California, United  
14 States of America

15 <sup>6</sup>Department of Statistics, Virginia Polytechnic and State University, 250 Drillfield Drive,  
16 Blacksburg, Virginia, United States of America

17 \*These authors share lead author status and contributed equally.

18 † **Corresponding author:** [sjryan@ufl.edu](mailto:sjryan@ufl.edu)

19

20

21 **Abstract:** Forecasting the impacts of climate change on *Aedes*-borne viruses—especially  
22 dengue, chikungunya, and Zika—is a key component of public health preparedness We apply an  
23 empirically parameterized Bayesian model of *Aedes*-borne viruses as a function of temperature  
24 to predict cumulative monthly global transmission risk in current climates, and compare against  
25 projected risk in 2050 and 2070 based on general circulation models (GCMs). Our results show  
26 that shifting suitability will track optimal temperatures for transmission (26-29 °C), potentially  
27 leading to poleward shifts. Furthermore, especially for *Ae. albopictus*, extreme temperatures are  
28 likely to limit transmission risk in current zones of endemicity, especially the tropics. The  
29 patterns of impact of changing minimum and maximum predicted temperatures lead to  
30 idiosyncratic outcomes for people at risk in the future. Validating these results with observed  
31 epidemic dynamics in upcoming decades will be paramount if global public health infrastructure  
32 is expected to keep pace with expanding vector-borne disease.

33 Climate change is likely to have a profound effect on the global distribution and burden of  
34 infectious diseases<sup>1-3</sup>. Current knowledge suggests that mosquito-borne diseases could expand  
35 dramatically in response to climate change<sup>4,5</sup>. However, the physiological and epidemiological  
36 relationships between mosquito vectors and the environment are complex and often non-linear,  
37 and experimental work has showed an idiosyncratic relationship between warming temperatures  
38 and disease transmission<sup>6,7</sup>. Accurately forecasting the potential impacts of climate change on  
39 *Aedes*-borne viruses—especially dengue, chikungunya, and Zika—thus becomes a key problem  
40 for public health preparedness<sup>4,8,9</sup>.

41 The intensification and expansion of vector-borne disease is likely to be one of the most  
42 significant threats posed by climate change to human health<sup>2,10</sup>. Mosquito vectors are of special  
43 concern, due to the global morbidity and mortality from diseases like malaria and dengue fever,  
44 as well as the prominent public health crises caused by (or feared from) several recently-  
45 emergent viral diseases like West Nile, chikungunya, and Zika. The relationship between climate  
46 change and mosquito-borne disease is perhaps best studied, in both experimental and modeling  
47 work, for malaria, and its associated *Anopheles* vectors. While climate change could exacerbate  
48 the burden of malaria at local scales, more recent evidence challenges the “warmer-sicker world”  
49 expectation<sup>11</sup>. The optimal temperature for malaria transmission has recently been demonstrated  
50 to be much lower than previously expected<sup>12</sup>, likely leading to net decreases in suitable habitat at  
51 continental scales in the coming decades<sup>13</sup>.

52 Relative to malaria, comparatively less is known about the net impact of climate change  
53 on *Aedes*-borne diseases. At a minimum, the distribution of *Aedes* mosquitoes is projected to  
54 shift in the face of climate change, with a mix of expansions in some regions and contractions in  
55 others, and no overwhelming net global pattern of gains or losses<sup>3,8</sup>. The consequences of those

56 range shifts for disease burden are therefore likely to be important, but can be challenging to  
57 summarize across landscapes and pathogens. Of all *Aedes*-borne diseases, dengue fever has been  
58 most frequently modeled in the context of climate change, and several models of the potential  
59 future of dengue have been published over the last two decades, with limited work building  
60 consensus among them<sup>4</sup>. Models relating temperature to vectorial capacity (the number of new  
61 infectious mosquito bites generated from a human case), and applying general circulation models  
62 (GCMs) to predict the impacts of climate change, go back as far as the late 1990s<sup>5</sup>. A study from  
63 2002 estimated that the population at risk (PAR) from dengue would rise from 1.5 billion in  
64 1990, to 5-6 billion by 2085, as a result of climate change<sup>14</sup>. A more recent study suggested that  
65 climate change alone should increase the global dengue PAR by 0.28 billion by 2050, but  
66 accounting for projected changes in global economic development (using GDP as a predictor for  
67 dengue risk) surprisingly reduces the projected PAR by 0.12 billion over the same interval<sup>15</sup>.  
68 Mechanistic models have shown that increases or decreases in dengue risk can be predicted for  
69 the same region based on climate models, scenario selection, and regional variability<sup>16</sup>.

70 Chikungunya and Zika viruses, which have emerged more recently as a public health  
71 crisis, are less well-studied in the context of climate change. A monthly model for chikungunya  
72 in Europe, constrained by the presence of *Ae. albopictus*, found that the A1B and B1 scenarios  
73 both correspond to substantial increases in chikungunya risk surrounding the Mediterranean<sup>17</sup>. A  
74 similar modeling study found that dengue is likely to expand far more significantly due to  
75 climate change than Zika<sup>9</sup> (though epidemiological differences among these three viruses remain  
76 unresolved<sup>18-20</sup>). However, the combined role of climate change and El Niño has already been  
77 suggested as a possible driver of the 2016 Zika pandemic's severity<sup>9</sup>. Global mechanistic  
78 forecasts accounting for climate change are all but nonexistent for both diseases, given how

79 recently both emerged as public health crises, and how much critical information is still lacking  
80 in the basic biology and epidemiology of both pathogens.

81 In this study, we apply a new mechanistic model of the spatiotemporal distribution of  
82 *Aedes*-borne viral outbreaks to resolve the role climate change could play in global transmission  
83 of dengue, chikungunya, and Zika. Whereas other mechanistic approaches rely on methods like  
84 dynamic energy budgets to build complex biophysical models for *Aedes* mosquitoes<sup>21,22</sup>, and  
85 subsequently (sometimes) extrapolate potential epidemiological dynamics<sup>5</sup>, our approach uses a  
86 single basic cutoff for the thermal interval where viral transmission is possible. The simplicity  
87 and transparency of the method masks a sophisticated underlying model that links the basic rate  
88 of reproduction  $R_0$  for *Aedes*-borne viruses to temperature, via experimentally-determined  
89 physiological response curves for traits like biting rate, fecundity, mosquito lifespan, extrinsic  
90 incubation rate, and transmission probability. The model is easily projected into geographic  
91 space by defining model based measures of suitability and classifying each location in space as  
92 suitable or not. We take a Bayesian approach in order to take into account uncertainty in the  
93 experimental data. We determine our suitability thresholds for transmission by calculating the  
94 temperature values at which the posterior probability that  $R_0 > 0$  exceeds 97.5%. For *Aedes*  
95 *aegypti*, these bounds are 21.3—34.0 °C, and for *Aedes albopictus*, 19.9—29.4 °C. This  
96 threshold condition defines the temperatures at which transmission is not prevented, rather than  
97 the more familiar threshold at which disease invasion is expected ( $R_0 > 1$ , which cannot be  
98 predicted in the absence of additional information on vector and human population sizes and  
99 other factors). We then classify each location by suitability in each month based on already  
100 published projections for current climates in the Americas<sup>6</sup>. Here, we expand the framework for  
101 both *Ae. aegypti* and *Ae. albopictus* to project cumulative months of suitability in current and

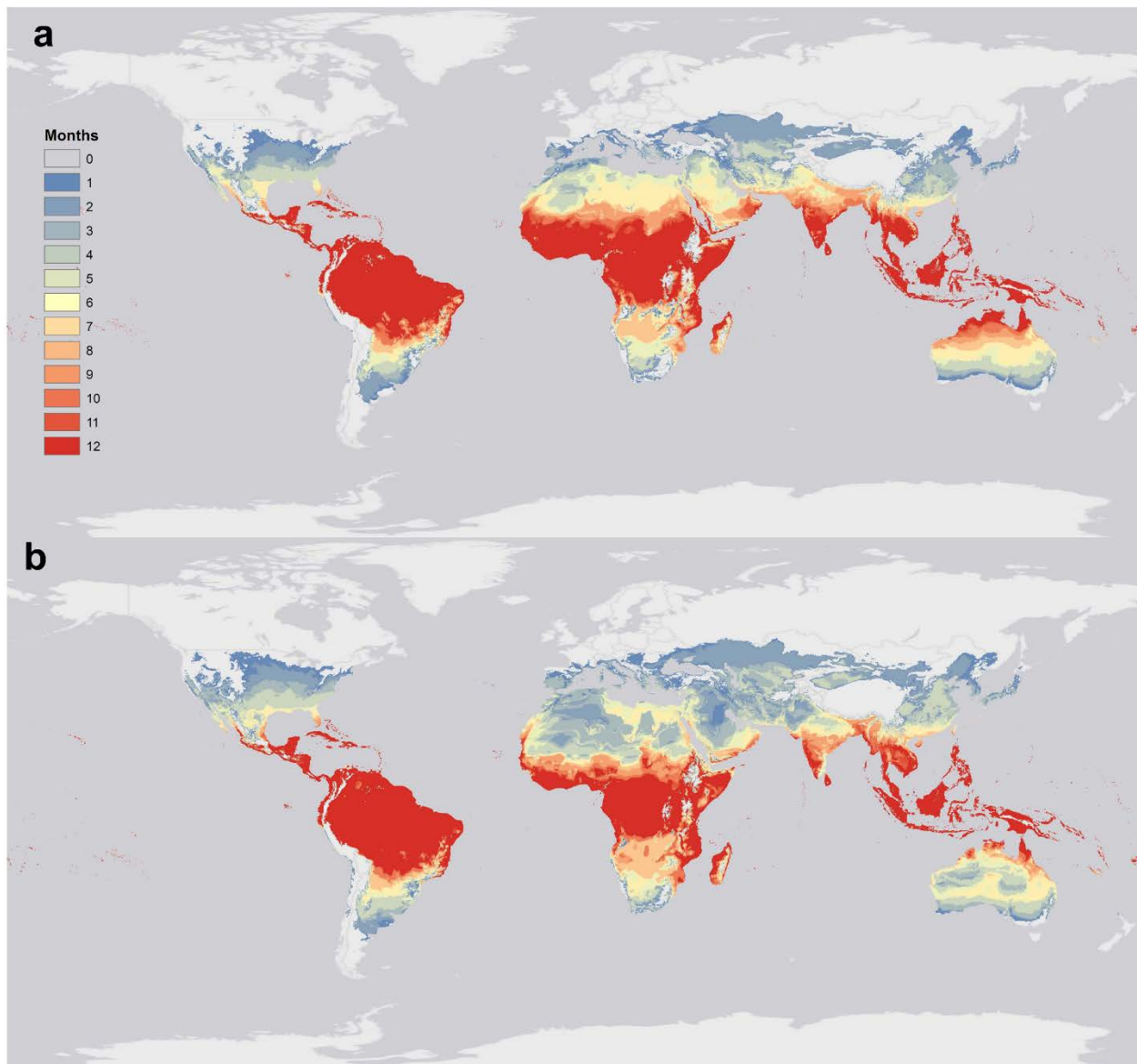
102 future (2050 and 2070) climates, and further examine how global populations at risk might  
103 change in different climate change scenarios. In doing so, we provide the first mechanistic  
104 forecast for the potential future transmission risk of chikungunya and Zika, which have been  
105 forecasted primarily via phenomenological methods (like ecological niche modeling<sup>9</sup>). Our study  
106 is also the first to address the seasonal aspects of population at risk for *Aedes*-borne diseases in a  
107 changing climate.

108 We found that the current pattern of suitability suggested by our model based on mean  
109 monthly temperatures (**Figure 1**) reproduces the known or projected distributions of dengue<sup>23</sup>,  
110 chikungunya<sup>24</sup>, and Zika<sup>9,25,26</sup> well. For both *Ae. aegypti* and *Ae. albopictus*, most of the tropics  
111 is currently optimal for viral transmission year-round, with suitability declining along latitudinal  
112 gradients. Many temperate regions are suitable for up to 6 months of the year currently, but  
113 outside the areas mapped as “suitable” by previous disease-specific distribution models; in some  
114 cases, limited outbreaks may only happen when cases are imported from travelers (e.g. in  
115 northern Australia, where dengue is not presently endemic but outbreaks happen in suitable  
116 regions<sup>16</sup>; or in mid-latitude regions of the United States, where it has been suggested that  
117 traveler cases could result in limited autochthonous transmission<sup>25,27</sup>).

118

119

120 **Figure 1 | Mapping current transmission risk.** Maps of current monthly suitability based on  
121 mean temperatures for a temperature suitability threshold corresponding to the posterior  
122 probability that scaled  $R_0 > 0$  is 97.5% for (a) *Aedes aegypti* and (b) *Aedes albopictus*.  
123

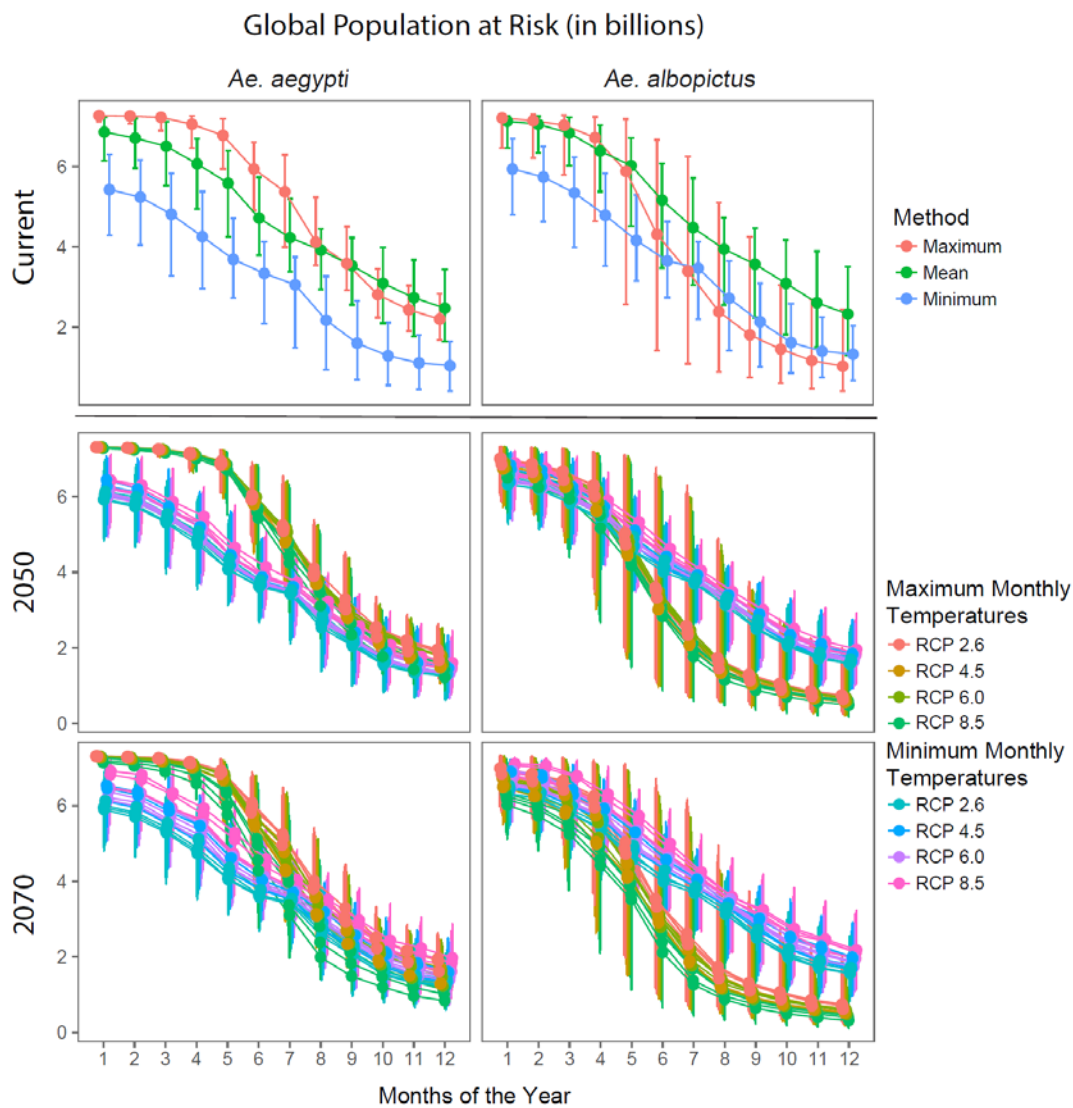


124

125 Transmission models in current climates, and derived maps of seasonal population at risk,  
126 were extremely sensitive to whether minimum, mean, or maximum monthly temperatures were  
127 used (**Figure S1-4**). Under current climates, maximum temperatures predict a consistently worse  
128 pattern of population-at-risk (PAR) from *Ae. aegypti* than minimum temperatures. For *Ae.*  
129 *albopictus*, the pattern is less straightforward, with maximum temperatures predicting the worst

130 outcome (highest number of people at risk) for shorter periods, but with minimum temperatures  
131 producing a worse pattern of risk measured by 6 or more months of suitability (**Figure 2**).

132 **Figure 2 | Current and future global population-at-risk.** Values correspond to population at  
133 risk for a given minimum number of months. Points correspond to the 50% posterior probability  
134 that scaled  $R_0 > 0$ , while confidence intervals correspond to probabilities of 2.5% and 97.5%.  
135 Left and right: *Aedes aegypti* and *Aedes albopictus*. Current models are separated by mosquito  
136 and by monthly minimum, mean, or maximum temperature; future model colors also reflect  
137 representative concentration pathways (RCPs) and minimum vs. maximum monthly temperature  
138 (see legend), while contrasting GCMs are plotted as separate trajectories with the same plotting  
139 scheme.



140



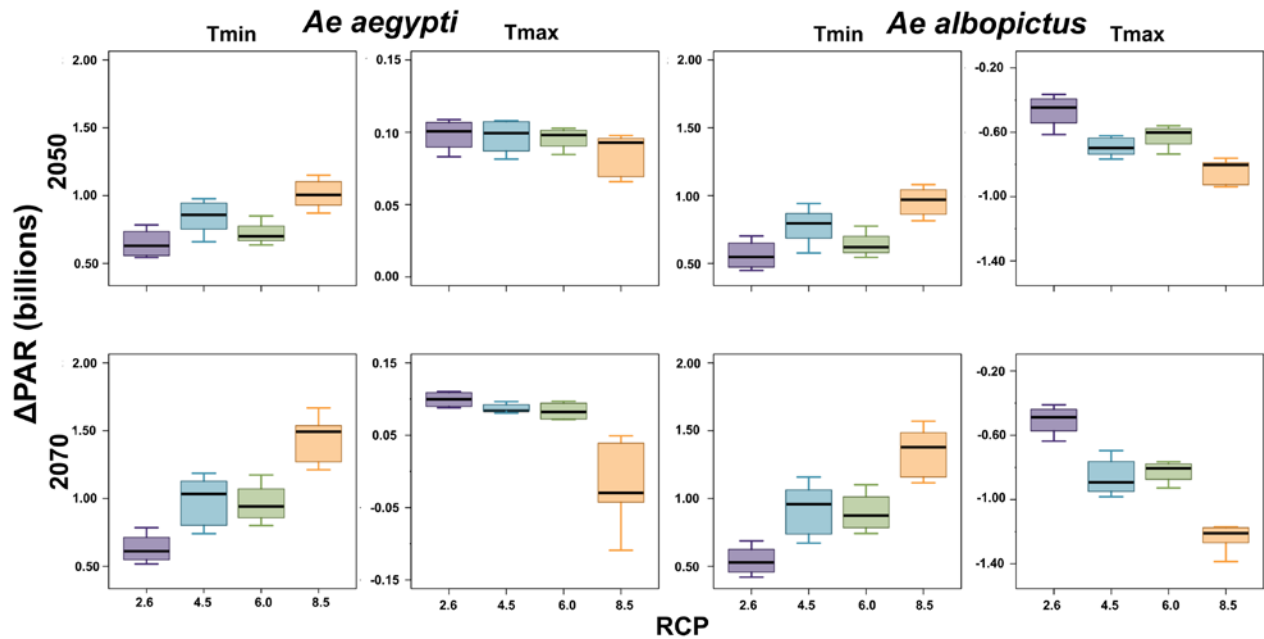
141 Perhaps most compelling, transmission curves generated by mean temperatures do not  
142 align neatly with either maximum or minimum curve, potentially demonstrating a downside of  
143 disease forecasts that do not account for the extreme ends of normal temperature variation.  
144 Resolving uncertainty in future climate-based disease forecasts requires resolving how  
145 temperature regimes as a whole (encapsulated by minimum, mean, and maximum monthly  
146 temperatures) translate into transmission potential.

147 The most surprising result of our study is that the upper thermal bound of *Aedes* viral  
148 transmission is likely to be increasingly relevant in a changing climate—even in localities with  
149 current year-round transmission. For *Ae. aegypti*, minimum temperatures produce far lower total  
150 extents of transmission, though the extent of year-round transmission is roughly comparable; the  
151 pattern is reversed for *Ae. albopictus*, for which the cumulative extent is the same, but minimum  
152 monthly temperatures predict year-round transmission risk for 1-2 billion more people (**Figure**  
153 **2**).

154 This is ultimately an emergent property of the same seasonal risk curves generated for  
155 current temperatures, and has key implications for interpreting the climate-disease relationship.  
156 (In particular, partial mitigation of climate change could keep *Ae. albopictus* mosquitoes  
157 especially within optimal thermal ranges for more of the year, and thereby produce worse  
158 clinical outcomes). Furthermore, for both mosquitoes, inter-annual and intra-monthly variation in  
159 weather may also have a more significant effect on viral outbreak outcomes than subtler  
160 variations in overall climate trends. Increasing climate change severity increases population at  
161 risk for both mosquitoes when using minimum temperatures but decreases it for *Ae. albopictus*  
162 transmission, using maximum temperatures (**Figure 3**). Moreover, the range of temperatures

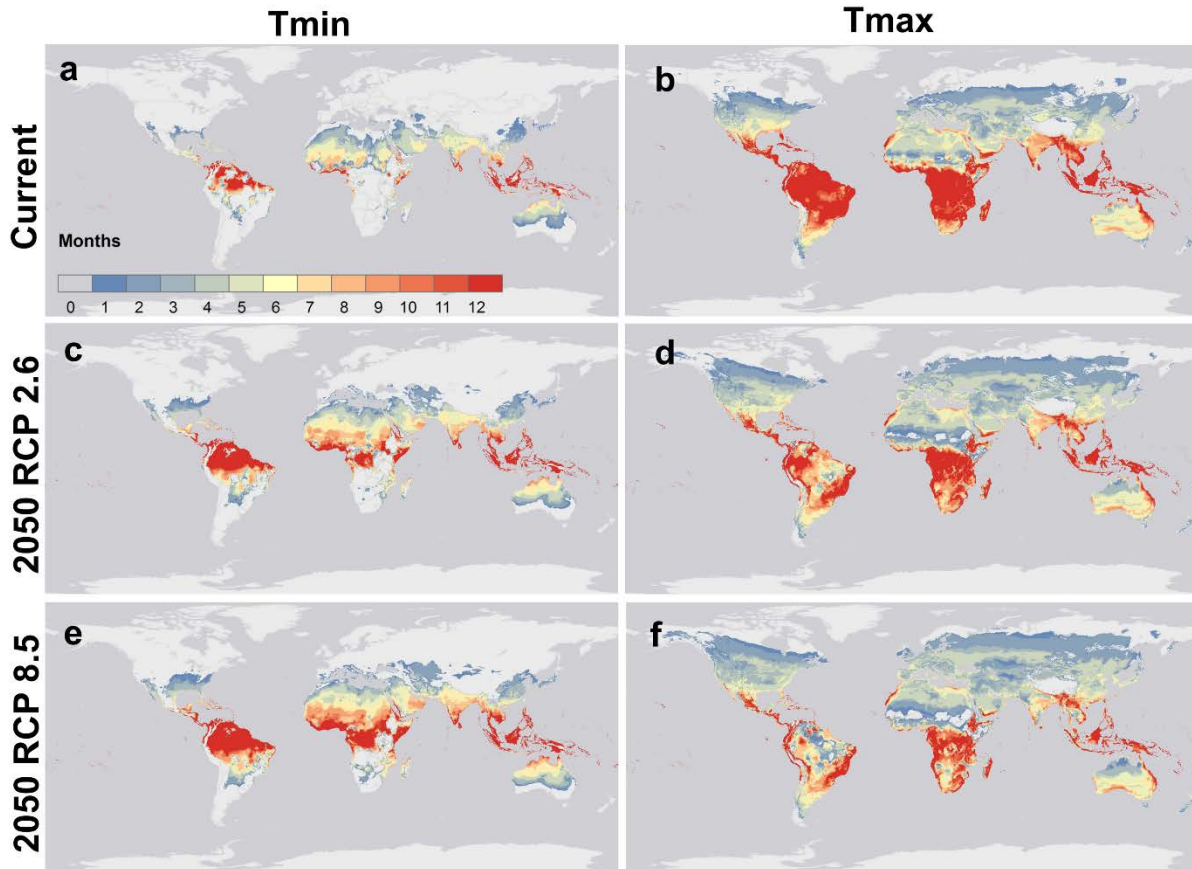
163 forecasted for a given month across scenarios produce a more dramatic range of risk forecasts  
164 than any combination of climate models and pathways.

165 **Figure 3** | Projected total changes in global population at risk (PAR, for one or more months),  
166 for *Aedes aegypti* and *Aedes albopictus* transmission, from current modeled PAR, as a function  
167 of minimum ( $T_{\min}$ ) and maximum ( $T_{\max}$ ) monthly temperatures, to 2050 (top row) and 2070  
168 (bottom row), by representative climate pathways (RCPs), across 4 general circulation models.



169 In the face of a changing climate, dramatic changes can be expected in the global  
170 spatiotemporal risk patterns from both *Ae. aegypti* (**Figure 4**) and *Ae. albopictus* (**Figure 5**). For  
171 minimum monthly temperatures, models for both mosquitoes in 2050 under the most and least  
172 optimistic pathways (RCPs 2.6 and 8.5) are quite different from current distributions, with the  
173 most notable changes being a southward shift of year-round suitable area in sub-Saharan Africa,  
174 an increase in months of suitability over a larger area in the Americas, an increase in suitable  
175 area through southern Europe, and an expansion of the northern range limits of transmission for  
176 both Europe and North America. In contrast, for maximum temperature scenarios for 2050, much  
177 more idiosyncratic distributional patterns develop. Both mosquitoes gain significant ground  
178 towards the poles for at least a few months of the year.

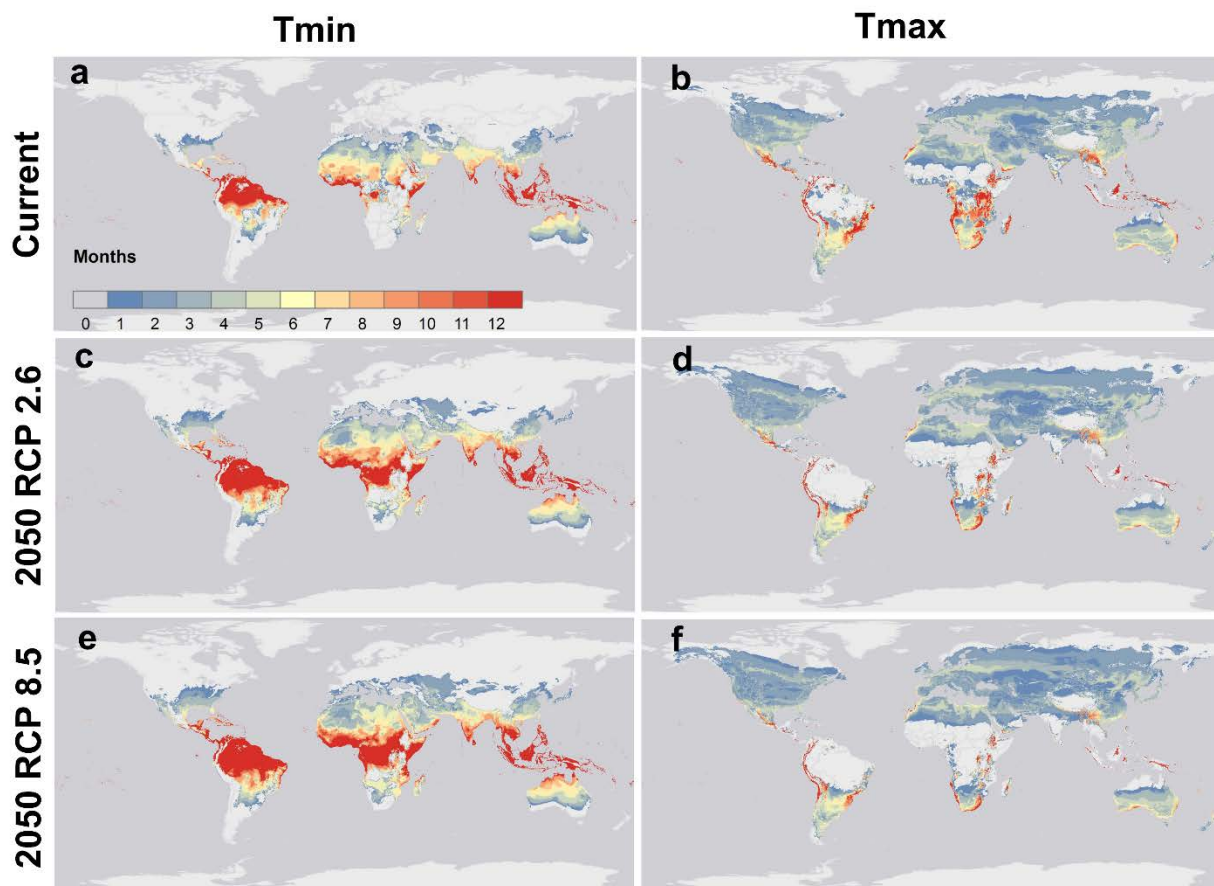
179 **Figure 4 | Mapping future transmission risk scenarios for *Aedes aegypti*.** Maps of monthly  
180 suitability based on a temperature threshold corresponding to the posterior probability that scaled  
181  $R_0 > 0$  is greater or equal to 97.5%, for transmission by *Aedes aegypti* for predicted minimum  
182 ( $T_{min}$ , Left - a,c,e) and maximum ( $T_{max}$ , Right - b,d,f) monthly temperatures under current (a,b)  
183 and future scenarios: HadGEM2-ES 2050 for RCP 2.6 (c,d) and RCP 8.5 (e,f).



184 In some cases, climate change is expected to reverse well-documented geographic  
185 patterns of transmission, like Australia's latitudinal gradient (with current transmission risk  
186 highest on the northern coast, but projected to shift towards the southern and eastern coasts by  
187 2050). While some core areas (like the Amazon or Indian subcontinent) become less suitable for  
188 year round transmission for *Ae. aegypti*, the overall pattern is one of expanding thermally-  
189 suitable area in sub-Saharan Africa, Central America, and the Andes. Whether this translates into  
190 increased vector establishment will depend heavily on land use patterns and urbanization at  
191 regional scales, a fact that may ultimately buffer some regions like the Andes from increased  
192 disease risk<sup>28,29</sup>. In contrast, for *Ae. albopictus*, future risk patterns change far more dramatically,

193 primarily because maximum temperature scenarios produce large reductions in range (**Figure 5**),  
194 corresponding to 1-2 billion fewer people at risk of year-round transmission even though the  
195 overall extent of suitability is roughly the same with minima and maxima (**Figure 2**). In the most  
196 extreme warming scenarios, the tropics become unsuitable year-round, with the only projected  
197 year-round transmission projected for high-elevation regions like the Andes mountains, or  
198 isolated patches of Africa and southeast Asia (**Figure 5**).

199 **Figure 5 | Mapping future transmission risk scenarios for *Aedes albopictus*.** Maps of monthly  
200 suitability based on a temperature threshold corresponding to the posterior probability that scaled  
201  $R_0 > 0$  is greater or equal to 97.5%, for transmission by *Aedes albopictus* for predicted minimum  
202 ( $T_{\min}$ , Left - a,c,e) and maximum ( $T_{\max}$ , Right - b,d,f) monthly temperatures under current (a,b)  
203 and future scenarios: HadGEM2-ES 2050 for RCP 2.6 (c,d) and RCP 8.5 (e,f).



204

205 Our model predicts that 6.1 billion people currently live in areas suitable for *Ae. aegypti*

206 transmission at least part of the year (i.e., 1 month or more) and 6.49 billion in areas suitable for

207 *Ae. albopictus* transmission (using mean temperatures). Whether future risk will be driven by  
208 rising minimum temperatures, moving people into suitable transmission temperatures, or instead  
209 maximum temperatures curbing transmission, as people are exposed to temperatures above  
210 suitable ranges, remains to be seen. However, we can anticipate each of these, using our  
211 modeling approaches, and see that they give us quite different predictions. Based on monthly  
212 minimum temperatures instead of means, there are currently 4.30 billion people at risk (PAR) in  
213 areas suitable for *Ae. aegypti* based transmission and 4.82 billion for *Ae. albopictus*. Under a  
214 minimum temperature projections, an average (across RCPs and GCMs) of 5.12 billion people  
215 live in areas facing increased exposure to climate suitability for *Ae. aegypti*-borne viruses by  
216 2050, and 5.57 billion for *Ae. albopictus*-borne viruses by 2050,. It is important to note that these  
217 changes represent shifts in location of suitable climates, so new individuals will become  
218 exposed, while others will see decreasing risk. A total of 85 thousand people live in areas likely  
219 to experience *decreased* climate suitability for exposure to transmission by *Ae. aegypti* by 2050  
220 (585 thousand by 2070), and a surprising 234 million for *Ae. albopictus* by 2050 (387 million by  
221 2070). Interestingly, by 2070, under minimum temperature change, 21 thousand people are  
222 predicted to entirely escape viral transmission by *Ae. aegypti*, and 28 thousand by *Ae. albopictus*.

223 Predicted monthly maximum temperatures lead to more dramatic predictions: currently,  
224 there are 7.15 billion people at risk (PAR) in areas suitable for *Ae. aegypti* based and 6.49 billion  
225 for *Ae. albopictus*. An average of 7.24 billion people face increased exposure to climate  
226 suitability for *Ae. aegypti*-borne viruses by 2050, and 5.82 billion for *Ae. albopictus*. By 2050,  
227 2.8 billion people live in areas likely to experience *decreased* climate suitability for exposure to  
228 transmission by *Ae. aegypti*, and 3.9 billion for *Ae. albopictus*. Under a maximum temperature

229 change scenario, 69 million people live in areas predicted to entirely escape viral transmission by  
230 *Ae. aegypti*, and 922 million are likely to escape *Ae. albopictus* transmission, by 2070.

231         These decreases suggest that climate change may not cause a direct global spike in  
232 *Aedes*-borne disease numbers, and could ultimately mitigate it; however, gains in exposure may  
233 have a more visible effect than losses, on realized disease outcomes, given the potential for  
234 explosive outbreaks (like Zika in the Americas) when viruses are first introduced into naïve  
235 populations<sup>30</sup>. The emergence of a Zika pandemic in the Old World, of chikungunya in Europe<sup>17</sup>,  
236 or of dengue anywhere the virus (or any given serotype) is not endemic, is still a critical concern.  
237 Whereas the highest predicted risk consistently occurs in south and southeast Asia, the most  
238 significant hotspots of *uncertainty* in our seasonal population at risk maps is evident in Europe  
239 and sub-Saharan Africa (**Figure S5, S6**), and we suggest that these especially require further,  
240 locally-tailored investigation by public health researchers.

241         While climate change poses perhaps the most serious growing threat to global health  
242 security, the relationship between climate change and worsening clinical outcomes for *Aedes*-  
243 borne diseases is unlikely to be straightforward. In practice, shifting patterns of suitability will  
244 correspond to different local patterns of exposure in a changing climate, independent of broader  
245 geographic constraints. The link from transmission risk to clinical outcomes is confounded by  
246 other health impacts of climate change, including changing precipitation patterns, socioeconomic  
247 development, changing patterns of land use and urbanization, potential vector (and virus)  
248 evolution and adaptation to warming temperatures, and changing healthcare landscapes, all of  
249 which covary strongly (potentially leading to nonlinearities). Together these will determine the  
250 burden of *Aedes*-borne outbreaks. Moreover, human adaptation to climate change will matter just  
251 as much as mitigation in determining how risk patterns shift; for example, increased drought

252 stress will likely correspond to water storage that increases proximity to *Aedes* breeding  
253 habitat<sup>31</sup>. Our models only provide an outer spatiotemporal bound to where transmission of  
254 dengue, chikungunya, and Zika is thermally plausible; climate change is likely to change the  
255 risk-burden relationship at fine scales within those zones of transmission in nonlinear ways, such  
256 that areas with shorter seasons of transmission could still experience worse overall disease  
257 burdens, or vice versa. As *Aedes*-borne diseases shift, research building consensus between our  
258 models and others, that works towards refine risk assessments within experimentally-determined  
259 outer bounds is paramount<sup>32</sup>.

260

## 261 **Methods**

### 262 *The Bayesian Model*

263 Our study presents geographic projections of published experimentally-derived mechanistic  
264 models of viral transmission by *Aedes aegypti* and *Aedes albopictus*. The approach to fit the  
265 thermal responses in a Bayesian framework and combine them to obtain the posterior  
266 distribution of  $R_0$  as a function of these traits is described in detail in Johnson *et al.*<sup>7</sup> and the  
267 particular traits and fits for *Aedes aegypti* and *Ae. albopictus* are presented in Mordecai *et al.*<sup>33</sup>.  
268 Once we obtain our posterior samples for  $R_0$  as a function of temperature we can evaluate the  
269 probability that  $R_0 > 0$  ( $\text{Prob}(R_0 > 0)$ ) at each temperature, giving a distinct curve for each  
270 mosquito species. We then define cutoff of  $\text{Prob}(R_0 > 0) = \alpha$  to determine our estimates of the  
271 thermal niche. For all except Figure 2 we use  $\alpha = 0.975$ . This very high probability allows us to  
272 isolate a temperature window for which transmission is almost certainly not excluded. For Figure  
273 2, points correspond to  $\alpha = 0.5$  and the lower/upper error bars to  $\alpha = 0.975$  and 0.025  
274 respectively. Note that the smaller probability leads to larger population at risk estimates because

275 the lower cutoff results in a wider thermal niche (i.e., temperatures where there is even a small  
276 chance that transmission could be permitted).

### 277 *Current & Future Climates*

278 Current mean, maximum, and minimum monthly temperature data was derived from the  
279 WorldClim dataset ([www.worldclim.org](http://www.worldclim.org)).<sup>34</sup> For future climates, we selected general circulation  
280 models (GCMs) that are most commonly used by studies forecasting species distributional shifts,  
281 at a set of four representative concentration pathways (RCPs) that account for different global  
282 responses to mitigate climate change. These are the Beijing Climate Center Climate System  
283 Model (BCC-CSM1.1); the Hadley GCM (HadGEM2-CC and HadGEM2-ES); and the National  
284 Center for Atmospheric Research's Community Climate System Model (CCSM4). Each of these  
285 can respectively be forecasted for RCP 2.6, RCP 4.5, RCP 6.0 and RCP 8.5. RCP numbers  
286 correspond to increased radiation in W/m<sup>2</sup> by the year 2100, therefore expressing scenarios of  
287 increasing severity. (However, even these scenarios are nonlinear over time. For example, in  
288 2050, RCP 4.5 is a more severe change than 6.0; see **Figure 3**.) For future climate scenarios,  
289 only minimum and monthly maximum projected temperatures are available. For most  
290 visualizations presented in the main paper (Figures 3 & 4), we used the HadGEM2-ES model,  
291 the most commonly used GCM. The mechanistic transmission model was projected onto the  
292 climate data using the 'raster' package in R 3.1.1. Subsequent visualizations were generated in  
293 ArcMap.

### 294 *Population at Risk*

295 To quantify a measure of risk, comparable between current and future climate scenarios, we used  
296 population count data from the Gridded Population of the World, version 4 (GPW4)<sup>35</sup>, predicted  
297 for the year 2015. We selected this particular population product as it is minimally modeled *a*



298 *priori*, ensuring that the distribution of population on the earth's surface has not been predicted  
299 by modeled covariates that would also influence our mechanistic vector-borne disease model  
300 predictions. These data are derived from most recent census data, globally, at the smallest  
301 administrative unit available, then extrapolated to produce continuous surface models for the  
302 globe for 5-year intervals from 2000-2020. These are then rendered as globally gridded data at  
303 30 arc-seconds; we aggregated these in R (raster<sup>30</sup>) to match the climate scenario grids at 5  
304 minute resolution (approximately 10km<sup>2</sup> at the equator). We used 2015 population count as our  
305 proxy for current, and explored future risk relative to the current population counts, for both  
306 minimum monthly temperature predictions, and maximum monthly temperature predictions.  
307 This prevents arbitrary demographic model-imposed patterns emerging, possibly obscuring  
308 climate generated change. We note that these count data reflect the disparities in urban and rural  
309 patterns appropriately for this type of analysis, highlighting population dense parts of the globe.  
310 Increasing urbanization would likely amplify the patterns we see, as populations increase overall,  
311 and the lack of appropriate population projections at this scale for 30-50 years in the future  
312 obviously limits the precision of the forecasts we provide.

313

#### 314 **Acknowledgements**

315 This work was funded by the National Science Foundation (DEB-1518681 to SJR, LRJ, EAM,  
316 NSF DEB-1641145 to SJR, and DEB-1640780 to EAM), the Stanford Woods Institute for the  
317 Environment ([https:// woods.stanford.edu/research/environmental- venture-projects](https://woods.stanford.edu/research/environmental-venture-projects)), and the  
318 Stanford Center for Innovation in Global Health ([http://globalhealth. stanford.edu/research/seed-](http://globalhealth.stanford.edu/research/seed-grants.html)  
319 [grants.html](http://globalhealth.stanford.edu/research/seed-grants.html)). Van Savage, Naveed Heydari, Jason Rohr, Matthew Thomas, and Marta Shocket  
320 provided helpful discussions on modeling approaches.

321

322 **Author Information**

323 The authors declare no competing interests. Correspondence and requests for materials should be  
324 addressed to S.J.R. ([sjryan@ufl.edu](mailto:sjryan@ufl.edu)).

325

326 **Author Contributions**

327 SJR initiated the idea for the study. SJR and LJ ran the models. CJC, SJR, EAM, and LJ wrote  
328 the manuscript. SJR and CJC made the figures.

329

330 **References**

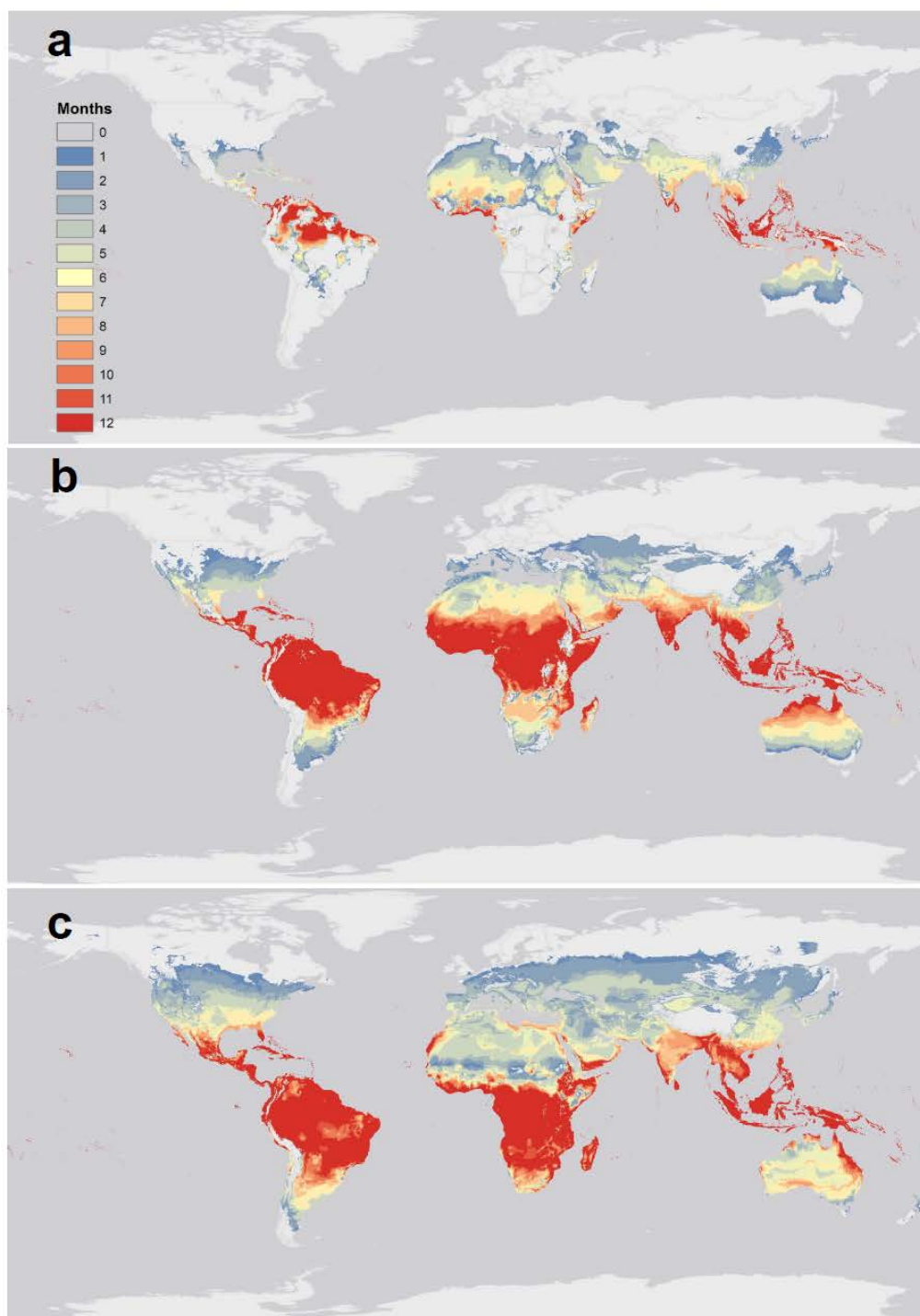
- 331 1. Hoberg, E. P. & Brooks, D. R. Evolution in action: climate change, biodiversity dynamics and  
332 emerging infectious disease. *Phil Trans R Soc B* **370**, 20130553 (2015).
- 333 2. Lafferty, K. D. The ecology of climate change and infectious diseases. *Ecology* **90**, 888–900  
334 (2009).
- 335 3. Escobar, L. E. *et al.* Declining Prevalence of Disease Vectors Under Climate Change. *Sci.*  
336 *Rep.* **6**, (2016).
- 337 4. Messina, J. P. *et al.* The many projected futures of dengue. *Nat. Rev. Microbiol.* **13**, 230–239  
338 (2015).
- 339 5. Patz, J. A., Martens, W., Focks, D. A. & Jetten, T. H. Dengue fever epidemic potential as  
340 projected by general circulation models of global climate change. *Environ. Health Perspect.*  
341 **106**, 147 (1998).
- 342 6. Mordecai, E. *et al.* Detecting the impact of temperature on transmission of Zika, dengue, and  
343 chikungunya using mechanistic models. *PLoS Negl. Trop. Dis.* **11**, e0005568 (2017).
- 344 7. Johnson, L. R. *et al.* Understanding uncertainty in temperature effects on vector-borne  
345 disease: a Bayesian approach. *Ecology* **96**, 203–213 (2015).
- 346 8. Campbell, L. P. *et al.* Climate change influences on global distributions of dengue and  
347 chikungunya virus vectors. *Phil Trans R Soc B* **370**, 20140135 (2015).
- 348 9. Carlson, C. J., Dougherty, E. R. & Getz, W. An ecological assessment of the pandemic threat  
349 of Zika virus. *PLoS Negl Trop Dis* **10**, e0004968 (2016).
- 350 10. Githeko, A. K., Lindsay, S. W., Confalonieri, U. E. & Patz, J. A. Climate change and vector-  
351 borne diseases: a regional analysis. *Bull. World Health Organ.* **78**, 1136–1147 (2000).

- 352 11. Ibelings, B. *et al.* Chytrid infections and diatom spring blooms: paradoxical effects of climate  
353 warming on fungal epidemics in lakes. *Freshw. Biol.* **56**, 754–766 (2011).
- 354 12. Mordecai, E. A. *et al.* Optimal temperature for malaria transmission is dramatically lower  
355 than previously predicted. *Ecol. Lett.* **16**, 22–30 (2013).
- 356 13. Ryan, S. J. *et al.* Mapping physiological suitability limits for malaria in Africa under climate  
357 change. *Vector-Borne Zoonotic Dis.* **15**, 718–725 (2015).
- 358 14. Hales, S., De Wet, N., Maindonald, J. & Woodward, A. Potential effect of population and  
359 climate changes on global distribution of dengue fever: an empirical model. *The Lancet* **360**,  
360 830–834 (2002).
- 361 15. AAström, C. *et al.* Potential distribution of dengue fever under scenarios of climate change  
362 and economic development. *Ecohealth* **9**, 448–454 (2012).
- 363 16. Williams, C. *et al.* Projections of increased and decreased dengue incidence under climate  
364 change. *Epidemiol. Infect.* 1–10 (2016).
- 365 17. Fischer, D. *et al.* Climate change effects on Chikungunya transmission in Europe: geospatial  
366 analysis of vector’s climatic suitability and virus’ temperature requirements. *Int. J. Health*  
367 *Geogr.* **12**, 51 (2013).
- 368 18. Funk, S. *et al.* Comparative analysis of dengue and Zika outbreaks reveals differences by  
369 setting and virus. *PLoS Negl. Trop. Dis.* **10**, e0005173 (2016).
- 370 19. Bastos, L. *et al.* Zika in Rio de Janeiro: assessment of basic reproductive number and its  
371 comparison with dengue. *BioRxiv* 055475 (2016).
- 372 20. Riou, J., Poletto, C. & Boëlle, P.-Y. A comparative analysis of Chikungunya and Zika  
373 transmission. *Epidemics* (2017).

- 374 21. Kearney, M., Porter, W. P., Williams, C., Ritchie, S. & Hoffmann, A. A. Integrating  
375 biophysical models and evolutionary theory to predict climatic impacts on species' ranges: the  
376 dengue mosquito *Aedes aegypti* in Australia. *Funct. Ecol.* **23**, 528–538 (2009).
- 377 22. Hopp, M. J. & Foley, J. A. Global-scale relationships between climate and the dengue fever  
378 vector, *Aedes aegypti*. *Clim. Change* **48**, 441–463 (2001).
- 379 23. Bhatt, S. *et al.* The global distribution and burden of dengue. *Nature* **496**, 504–507 (2013).
- 380 24. Nsoesie, E. O. *et al.* Global distribution and environmental suitability for chikungunya virus,  
381 1952 to 2015. *Euro Surveill. Bull. Eur. Sur Mal. Transm. Eur. Commun. Dis. Bull.* **21**, (2016).
- 382 25. Samy, A. M., Thomas, S. M., Wahed, A. A. E., Cohoon, K. P. & Peterson, A. T. Mapping  
383 the global geographic potential of Zika virus spread. *Mem. Inst. Oswaldo Cruz* **111**, 559–560  
384 (2016).
- 385 26. Messina, J. P. *et al.* Mapping global environmental suitability for Zika virus. *Elife* **5**, e15272  
386 (2016).
- 387 27. Bogoch, I. I. *et al.* Anticipating the international spread of Zika virus from Brazil. *Lancet*  
388 *Lond. Engl.* **387**, 335–336 (2016).
- 389 28. Grau, H. R. *et al.* The ecological consequences of socioeconomic and land-use changes in  
390 postagriculture Puerto Rico. *AIBS Bull.* **53**, 1159–1168 (2003).
- 391 29. Li, Y. *et al.* Urbanization increases *Aedes albopictus* larval habitats and accelerates mosquito  
392 development and survivorship. *PLoS Negl. Trop. Dis.* **8**, e3301 (2014).
- 393 30. Lucey, D. R. & Gostin, L. O. The emerging Zika pandemic: enhancing preparedness. *Jama*  
394 **315**, 865–866 (2016).
- 395 31. Beebe, N. W., Cooper, R. D., Mottram, P. & Sweeney, A. W. Australia's dengue risk driven  
396 by human adaptation to climate change. *PLoS Negl. Trop. Dis.* **3**, e429 (2009).

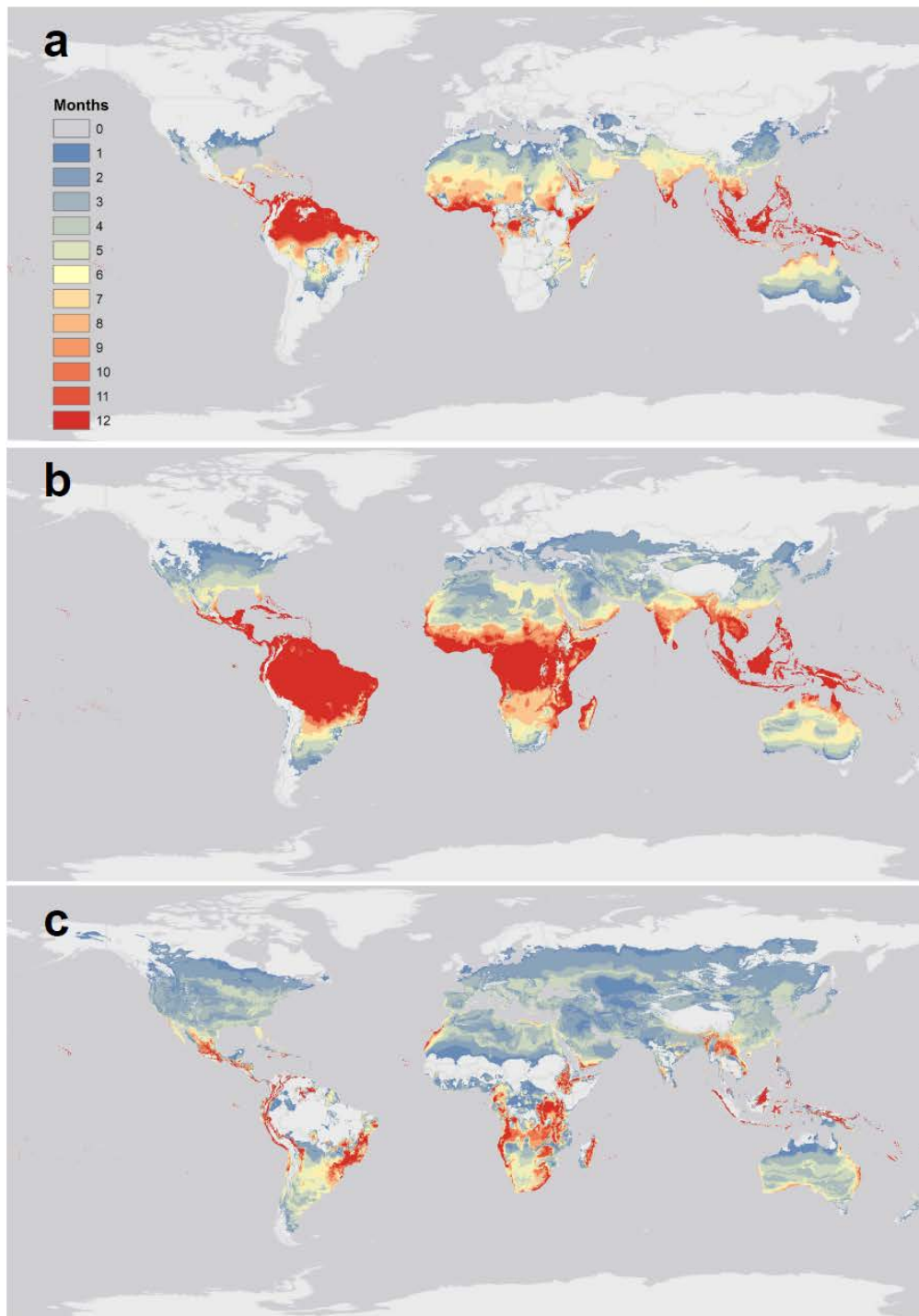
- 397 32. Carlson, C. J., Dougherty, E., Boots, M., Getz, W. & Ryan, S. Consensus and conflict among  
398 ecological forecasts of Zika virus outbreaks in the United States. *bioRxiv* 138396 (2017).
- 399 33. Mordecai, E. A. *et al.* Detecting the impact of temperature on transmission of Zika, dengue,  
400 and chikungunya using mechanistic models. *PLoS Negl. Trop. Dis.* **11**, e0005568 (2017).
- 401 34. Hijmans, R. J., Cameron, S. E., Parra, J. L., Jones, P. G. & Jarvis, A. Very high resolution  
402 interpolated climate surfaces for global land areas. *Int. J. Climatol.* **25**, 1965–1978 (2005).
- 403 35. Center for International Earth Science Information Network (CIESIN), Columbia University.  
404 *Gridded Population of the World, Version 4 (GPWv4)*. (US NASA Socioeconomic Data and  
405 Applications Center (SEDAC), 2016).
- 406 36. Hijmans, R. J. & van Etten, J. *raster: Geographic analysis and modeling with raster data*.  
407 (2012).
- 408

409 **Figure S1** | Current months of the year suitable for *Ae aegypti* transmission for (a) minimum, (b)  
410 mean, and (c) maximum monthly temperatures, where the posterior probability that scaled  $R_0 > 0$   
411 is greater or equal to 97.5%.



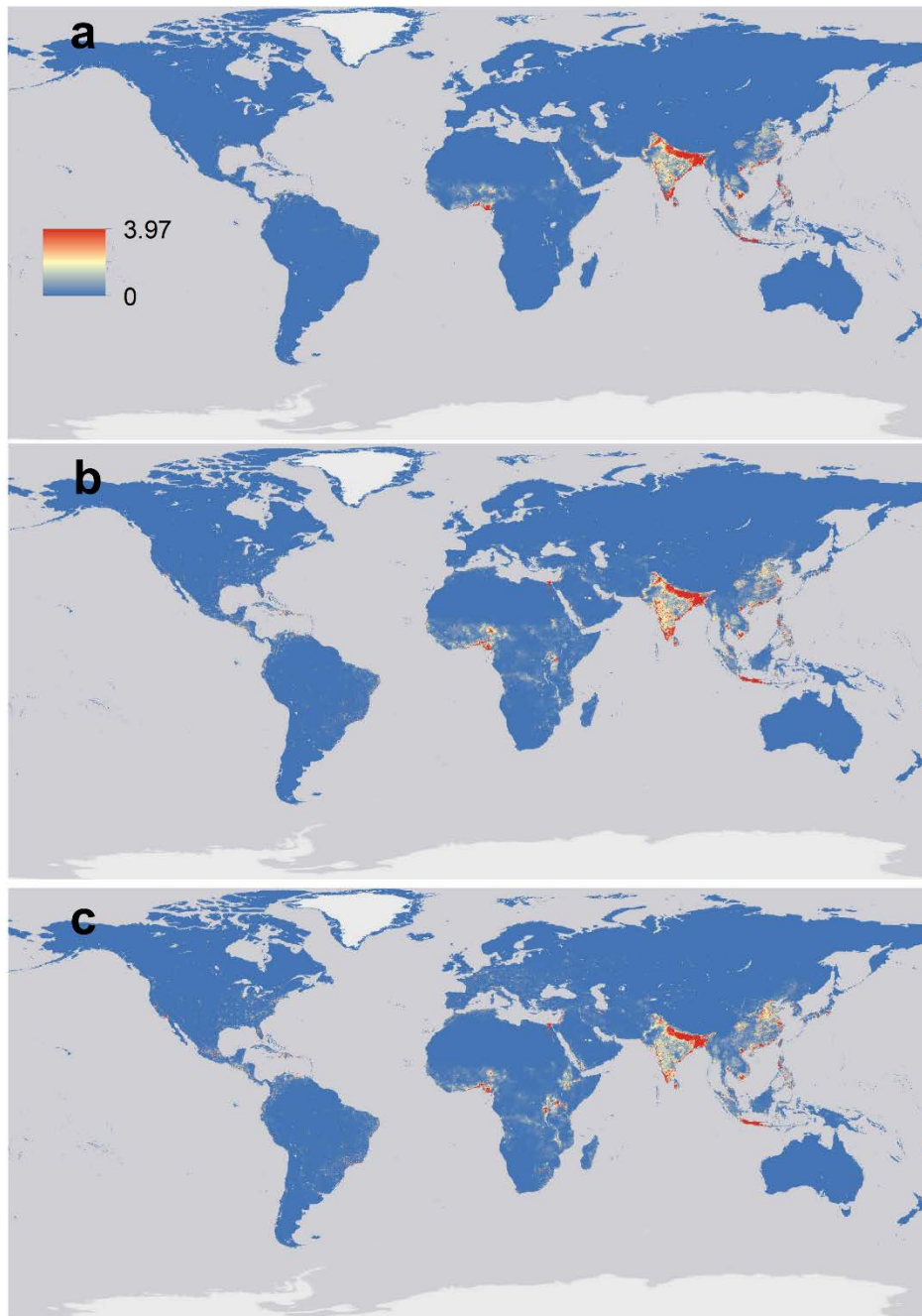
412

413 **Figure S2** | Current months of the year suitable for *Ae albopictus* transmission for (a) minimum,  
414 (b) mean, and (c) maximum monthly temperatures, where the posterior probability that scaled  $R_0$   
415  $> 0$  is greater or equal to 97.5%.



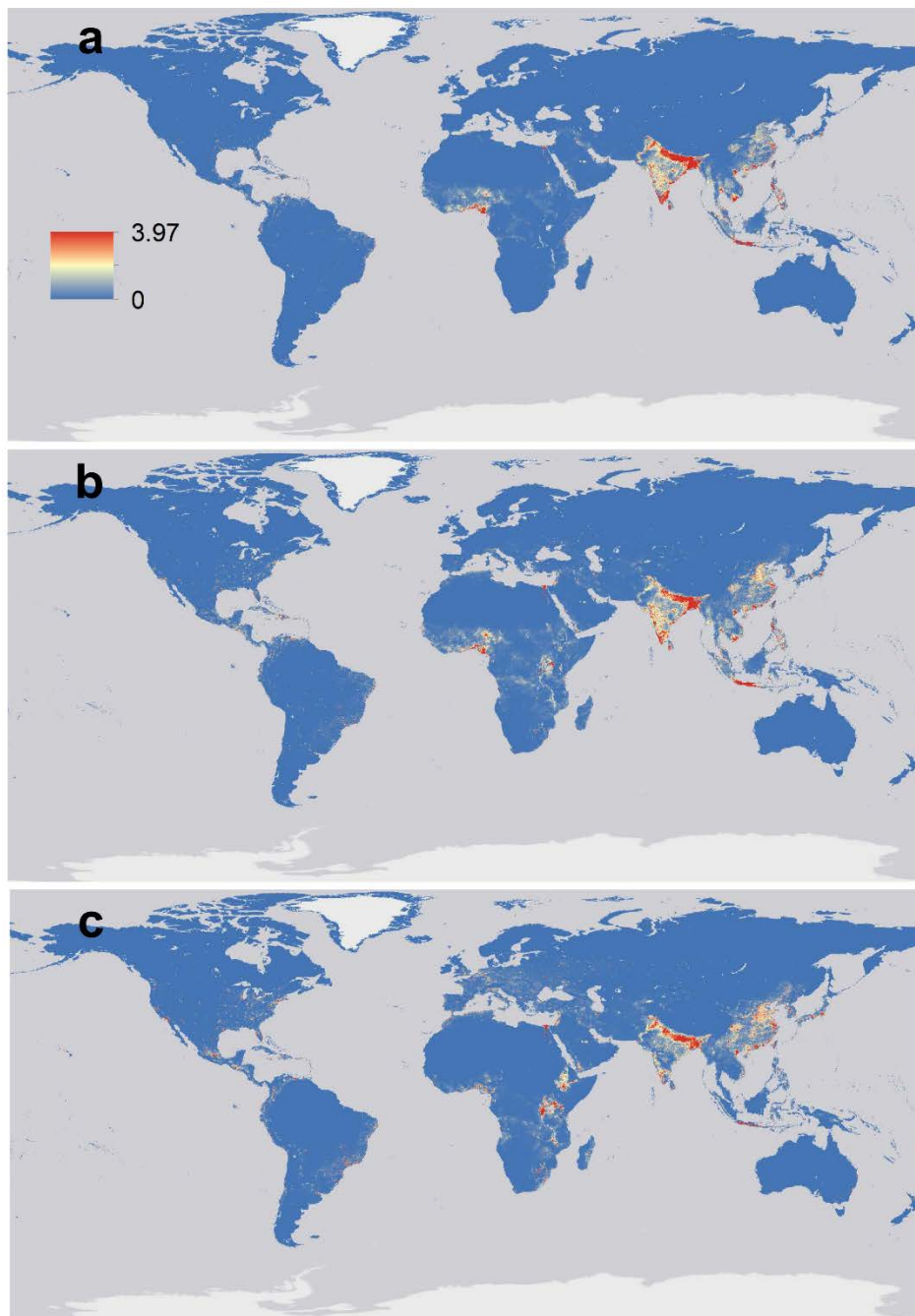


417 **Figure S3** | *Aedes aegypti* current mPAR (months\*people at risk), for (a) minimum, (b) mean,  
418 and (c) maximum temperature. The number of months of transmission suitability generated  
419 under current temperature models were multiplied by the estimated population for 2015 (Gridded  
420 Population of the World GPW4<sup>35</sup>).



421

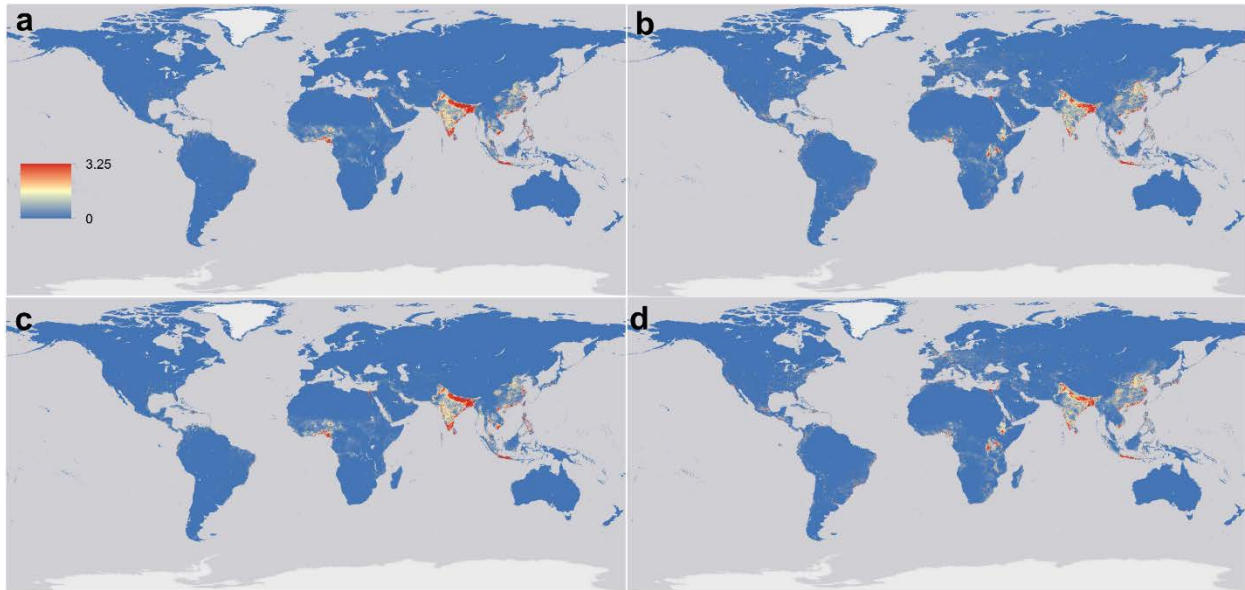
422 **Figure S4** | *Aedes albopictus* current mPAR (months\*people at risk), for (a) minimum, (b) mean,  
423 and (c) maximum temperature. The number of months of transmission suitability generated  
424 under current temperature models were multiplied by the estimated population for 2015 (Gridded  
425 Population of the World GPW4<sup>35</sup>).



426

427

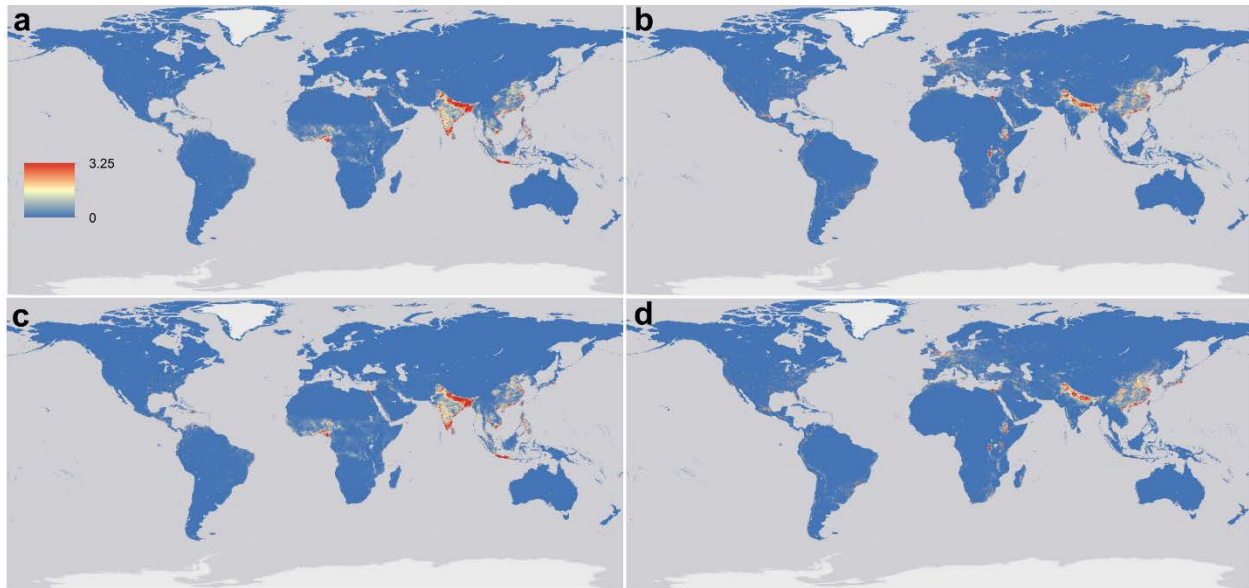
428 **Figure S5** | *Aedes aegypti* future mPAR (months\*people at risk), for (a) 2050 and (c) 2070 (max  
429 HadGEM2-ES RCP 8.5), versus the highest year-round PAR for (b) 2050 and (d) 2070 (max  
430 CCSM4 RCP 2.6). The number of months of transmission suitability generated under  
431 temperature models were multiplied by the estimated population for 2015 (Gridded Population of  
432 the World GPW4<sup>35</sup>).



433

434

435 **Figure S6** | *Aedes albopictus* future mPAR (months\*people at risk), for (a) 2050 and (c) 2070  
436 (max HadGEM2-ES RCP 8.5), versus the highest year-round PAR for (b) 2050 and (d) 2070  
437 (max CCSM4 RCP 2.6). The number of months of transmission suitability generated under  
438 temperature models were multiplied by the estimated population for 2015 (Gridded Population of  
439 the World GPW4<sup>35</sup>).



440